Articles

Synthesis of Nanowire and Hollow $LiFePO_4$ Cathodes for High-Performance Lithium Batteries

Sunhye Lim,[†] Chong S. Yoon,[‡] and Jaephil Cho*,[†]

Department of Applied Chemistry, Hanyang University, Ansan, Korea 426-791, and Division of Materials Science and Engineering, Hanyang University, Seoul, Korea 133-791

Received December 26, 2007. Revised Manuscript Received May 9, 2008

The synthesis of nanowire and hollow $LiFePO_4$ cathodes using the hard templates KIT-6 and SBA-15 is reported for high-performance lithium batteries. The two-dimensional hexagonal SBA-15 silica template with *P6mm* symmetry is used for the template that contains parallel cylindrical pores arranged with hexagonal symmetry, which serves to organize the wires into parallel bundles. On the other hand, three-dimensional cubic arrangement of pores in KIT-6 silica with *Ia3d* symmetry yields hollow morphology with mesopores. After impregnation of the template into a solution or after coating on the template with a solution consisting of $LiFePO_4$ precursors, the silica template is removed and is subsequently fired at 700 °C. Electrochemical cycling of both the nanowire and hollow $LiFePO_4$ cathodes demonstrates excellent rate capability even above 10C rate, showing >89% capacity retention of the initial capacity. Among them, the rate capability of the hollow cathode at 15C is higher than that of the nanowire cathode, showing 6% improvement due to its higher Brunauer−Emmett−Teller surface area.

1. Introduction

Recently, extensive study aimed at improving the high rate characteristics of the electrode materials for lithium batteries, such as TiO_2,[1–4] $Li_4Ti_5O_{12}$,[5] and $LiFePO_4$,[6–11] have been reported. Manipulation of these nanostructures provides versatile strategies toward improving the electrochemical properties. For example, TiO_2 prepared in a nanostructure showed significantly improved capacity retention at higher C rates.[1,2] However, lithium transition-metal oxides ($LiCoO_2$, $LiNi_{1-x}M_xO_2$) exhibited limited nanostructures.[12–14] In the case of $LiFePO_4$, due to its low intrinsic electronic conductivity (10^{-8} to 10^{-10} s/cm), studies on the utilization of the maximum specific capacity have been reported.[15–18] The marked increase in the rate capability of nanoscale doped $LiFePO_4$ was first reported by Chung et al.[19] They achieved >110 mA·h/g at 20C rate discharge at room temperature. Following this work, methods that increase the utilization of the $LiFePO_4$ capacity have been reported with only carbon or conducting polymer coatings or by control of the particle size.[21–27] Huang et al. reported that a composite of $LiFePO_4$ with a carbon xerogel that formed from a resorcinol-

* To whom correspondence should be addressed.
[†] Department of Applied Chemistry.
[‡] Division of Materials Science and Engineering.

(1) Armstrong, G.; Armstrong, A. R.; Canales, J.; Garcia, R.; Bruce, P. G. *Electrochem. Solid-State Lett.* **2006**, *9*, A139.
(2) Hu, Y.-S.; Kienle, L.; Guo, Y.-G.; Maier, J. *Adv. Mater.* **2006**, *18*, 1421.
(3) Sudant, G.; Baudrin, E.; Larcher, D.; Tarascon, J.-M. *J. Mater. Chem.* **2005**, *15*, 1263.
(4) Moriguchi, I.; Hidaka, R.; Yamada, H.; Kudo, T.; Murakami, H.; Nakashima, N. *Adv. Mater.* **2006**, *18*, 69.
(5) Kim, J.; Cho, J. *Electrochem. Solid-State Lett.* **2007**, *10*, A81.
(6) Chen, Z.; Dahn, J. R. *J. Electrochem. Soc.* **2002**, *149*, A1184.
(7) Dominko, D.; Gaberscek, M.; Drofenik, J.; Bele, M.; Jamnik, J. *Electrochim. Acta* **2003**, *48*, 2709.
(8) Dominko, R.; Bele, M.; Gaberscek, M.; Remskar, M.; Hanzel, D.; Pejovnik, S.; Jamnik, J. *J. Electrochem. Soc.* **2005**, *152*, A607.
(9) Lu, J.; Tang, Z.; Zhang, Z.; Shen, W. *J. Electrochem. Soc.* **2005**, *152*, A1441.
(10) Wang, G. X.; Yang, L.; Bewlay, S. L.; Chen, Y.; Liu, H. K.; Ahn, J. H. *J. Power Sources* **2005**, *146*, 521.
(11) Nakamura, T.; Miwa, Y.; Tabuchi, M.; Yamada, Y. *J. Electrochem. Soc.* **2006**, *153*, A1108.
(12) Cho, J.; Kim, Y.; Kim, M. G. *J. Phys. Chem. C* **2007**, *111*, 3192.
(13) Jiao, F.; Shaju, K. M.; Bruce, P. G. *Angew. Chem., Int. Ed.* **2005**, *44*, 6550.
(14) Park, D. H.; Lim, S. T.; Hwang, S.-J.; Yoon, C.-S.; Sun, Y.-K.; Choy, J.-H. *Adv. Mater.* **2005**, *17*, 2834.
(15) Liu, Y.; Dong, J.; Liu, M. *Adv. Mater.* **2004**, *16*, 353.
(16) (a) Hu, Y.-S.; Guo, Y.-G.; Dominko, R.; Gaberscek, M.; Jamink, J.; Maier, J. *J. Adv. Mater.* **2007**, *19*, 1963. (b) Park, K. S.; Schougaard, S. B.; Goodenough, J. B. *Adv. Mater.* **2007**, *19*, 848.
(17) Chung, S. Y.; Chiang, Y. M. *Nat. Mater.* **2003**, *1*, 123.
(18) (a) Huang, H.; Yin, S.-C.; Nazar, L. F. *Electrochem. Solid-State Lett.* **2001**, *4*, A170. (b) Ellis, B.; Kan, W. H.; Makahnouk, W. R.; Nazar, L. F. *J. Mater. Chem.* **2007**, *17*, 3249.
(19) Chung, S.-U.; Bloking, J. T.; Chiang, Y.-M. *Nat. Mater.* **2002**, *1*, 123.
(20) Xie, H.-M.; Wang, R.-S.; Ying, J.-R.; Zhang, L.-Y.; Jalbout, A. F.; Tu, H.-Y.; Yang, G.-L.; Pan, X.-M.; Su, Z.-M. *Adv. Mater.* **2006**, *18*, 2609.
(21) Kim, D.-H.; Kim, J. *Electrochem. Solid-State Lett.* **2006**, *9*, A439.
(22) Wang, B.; Qiu, Y.; Yang, L. *Electrochem. Commun.* **2006**, *8*, 1801.
(23) Croce, F.; Epifanio, A. D.; Hassoun, J.; Deptula, A.; Olezac, T.; Scrosati, B. *Electrochem. Solid-State Lett.* **2002**, *5*, A47.
(24) Higuchi, M.; Kayayama, K.; Azuma, Y.; Yukawa, M.; Schara, M. *J. Power Sources* **2003**, *119*, 258.
(25) Bauer, E. M.; Bellitto, C.; Pasquali, M.; Prosini, P. P.; Righini, G. *Electrochem. Solid-State Lett.* **2004**, *7*, A85.
(26) Delacourt, C.; Poizot, P.; Levasseur, S.; Masquelier, C. *Electrochem. Solid-State Lett.* **2006**, *9*, A352.
(27) Yamada, A.; Yonemura, M.; Takei, Y.; Sonoyama, N.; Kanno, R. *Electrochem. Solid-State Lett.* **2005**, *8*, A55.

10.1021/cm8006364 CCC: $40.75
Published on Web 06/20/2008

formaldehyde precursor showed ~150 mA·h/g at a rate of 0.2C and 110 mA·h/g at a rate of 5C.[18] Xie et al. reported that a $LiFePO_4$−PAS composite showed an initial discharge capacity of 150 and 100 mA·h/g at a rate of 5C under a 3−5 mg/cm^2 loading level.[20] More recently, works on $LiFePO_4$, such as mechanism of Fe^{3+} reduction at low temperature,[28] enhanced rate capability by a carbon nanotube coating[29] or wired pore formation,[30] and high-resolution electron energy loss spectroscopy,[31] were reported.

In spite of many studies that centered on the preparation of metal oxide derivatives using a hard-template,[32–39] the synthesis of nanowire and hollow $LiFePO_4$ has not been reported in the open literature. In the present study, the synthesis of nanowire and hollow $LiFePO_4$ cathodes using the hard templates KIT-6 and SBA-15 is reported. Even after removal of the template, such morphologies are maintained. Nanowire and hollow $LiFePO_4$ cathodes show excellent capacity retention even at a 15C rate, exceeding >85% capacity retention of the initial capacity.

2. Experimental Section

KIT-6 and SBA-15 were prepared in an aqueous solution using Pluronic P123 (EO20−PO70−EO20, MW = 5800, Aldrich) as a structure-directing agent according to Choi's work and others.[40,41] TEOS (Aldrich, 98%) was used as the silica precursor. The fired SiO_2 powders at 500 °C were used as a template for synthesizing nanowires and hollow $LiFePO_4$. For a typical synthesis of a nanowire sample, 12.8 g of $Fe(NO_3)_3 \cdot 9H_2O$ (Junsei, 99%), 3.23 g of $LiC_2H_3O_2 \cdot 2H_2O$ (Aldrich, 99.9%), and 3.10 g of H_3PO_4 (Aldrich, 99%) were dissolved in 20 mL of ethanol. This transparent solution was incorporated into 1.7 g of hexagonal SBA-15 silica powder using a wetness impregnation technique. After the impregnated sample was dried in an oven at 120 °C, the powders were impregnated again using the same method described above. The $LiFePO_4$ precursor/SiO_2 composite was annealed at 300 °C for 3 h, and the silica template was removed from the composite by rinsing with 1 M NaOH solution. After removal of the SiO_2 template, the $LiFePO_4$ was rinsed with water several times and dried at 100 °C overnight. Finally, it was fired at 700 °C under a mixed gas (90% N_2 and 10% H_2) flow for 5 h. For preparation of the hollow $LiFePO_4$, the same experimental method as above was used except for the use of KIT-6 template and the viscous solution after heating of the transparent solution at 40 °C. This viscous transparent solution was coated onto 1.7 g of hexagonal KIT-6 silica powder and dried at 120 °C using a coating method reported by Cho and co-workers.[42,43] The remaining process is identical to that described for obtaining nanowire $LiFePO_4$. CHNS-elemental analyzer (Shimadzu) was used to get quantitative information of the carbon contents of the samples, and its content of the nanowire and hollow samples was estimated to 0.41 and 0.43 wt %, respectively.

Cathode electrodes were constructed by mixing the cathode powders, polyvinylidene binder, and Super P carbon black at a weight ratio of 80:10:10 in a NMP solvent. The mixed slurry was cast onto Al foil with the slurry thickness controlled by a doctor-blade coater. After evaporation of the solvent at 130 °C for 20 min, the electrodes were pressed using a roll press. The electrodes were assembled into coin-type half-cells (2016R-type) with a Li electrode and ethyl carbonate/dimethyl carbonate (EC/DMC) (1:1 vol %) with 1 M $LiPF_6$ salt (Cheil Industries, Korea) in an Ar-filled glove box. The materials were then characterized by FE-TEM (JEOL 2010F) and XRD (Rigaku, 18 kW with Cu radiation). Transmission electron microscope (TEM) samples were prepared by the evaporation of the dispersed naoparticles in acetone or hexane on carbon-coated copper grids. TEM and high-resolution TEM (HRTEM) analysis were performed on a JEOL 2010F operating at 200 kV equipped with an energy-dispersive X-ray (EDX) spectrometer.

3. Results and Discussion

To prepare the nanowire $LiFePO_4$, a transparent mixed solution consisting of $LiFePO_4$ precursors was incorporated into a SBA-15 silica template using an impregnation method. However, a single impregnation did not result in fully grown nanowires, and after the third impregnation, a fully grown bundle of nanowires was observed (Figure 1A); its TEM image (Figure 1B) shows that the nanowires have a diameter of ~7 nm. An HREM image (Figure 1C) clearly shows the lattice fringes of the (200) and (201) planes corresponding to *d* spacing values of 5.2 and 3.0 Å of $LiFePO_4$. Although the wires are continuous (Figure 1A), close inspection of the high-resolution image (Figure 1C) indicates that the distance between the wires is irregular, and the nanowire consists of connected agglomerated nanoparticles in a single direction. Energy-dispersive X-ray spectra of different regions 1 and 2 confirm no traces of Na and Si impurities of the samples and the intensity ratios of the Fe, P, and O elements are very similar to each other. Further, ICP-MS (inductively coupled plasma-mass spectroscopy) confirmed the $Li_{0.99}FePO_4$ and showed residual Si and Na impurity of 19 and 25 ppm, respectively.

Figure 2A shows the typical Rietveld refinement result of the nanowire $LiFePO_4$ and all the peaks can be indexed on the basis of an orthorhombic olivine structure with a *Pnma* space group. Figure 2B shows an XRD diffraction pattern of the nanowire and hollow samples, and the Miller indices of the peaks are also indicated in the XRD pattern. The lattice constants of the nanowire sample were $a = 10.328(4)$, $b = 6.008(3)$, and $c = 4.703(4)$. Only the hollow sample shows the peak corresponding to Fe_2P phase with a detectable level, but it cannot rule out the possibility of the presence of the Fe_2P phase in the nanowire sample also. Moreover, since we used Li acetate as a precursor, there is the possibility of the formation of carbon on the final products. Carbon

(28) Ravet, N.; Gauthier, M.; Zaghib, K.; Goodenough, J. B.; Mauger, A.; Gendron, F.; Julien, C. M. *Chem. Mater.* **2007**, *19*, 2595.
(29) Kavan, L.; Exnar, I.; Cech, J.; Graetzel, M. *Chem. Mater.* **2007**, *19*, 4716.
(30) Dominko, R.; Bele, M.; Goupil, J.-M.; Gaberscek, M.; Hanzel, D.; Arcon, I.; Jamink, J. *Chem. Mater.* **2007**, *19*, 2690.
(31) Laffont, L.; Delacourt, C.; Gibot, P.; Wu, M. W.; Kooman, P.; Masquelier, C.; Tarascon, J.-M. *Chem. Mater.* **2007**, *18*, 5220.
(32) Caruso, F. *Adv. Mater.* **2001**, *13*, 11.
(33) Dhas, N. A.; Suslick, K. S. *J. Am. Chem. Soc.* **2005**, *127*, 2368.
(34) Vasquez, Y.; Sra, A. K.; Schaak, R. E. *J. Am. Chem. Soc.* **2005**, *127*, 12504.
(35) Tierno, P.; Goedel, W. A. *J. Phys. Chem. B* **2006**, *110*, 3043.
(36) Schüth, F. *Chem. Mater.* **2001**, *13*, 3184.
(37) Wang, Y.; Yang, C.-M.; Schmidt, W.; Spliethoff, B.; Bill, E.; Schüth, F. *Adv. Mater.* **2005**, *17*, 53.
(38) Xu, H.; Wang, W. *Angew. Chem., Int. Ed.* **2007**, *47*, 1489.
(39) Tian, B.; Liu, X.; Yang, H.; Xie, S.; Yu, C.; Zhao, D. *Adv. Mater.* **2003**, *15*, 1370.
(40) Choi, M.; Heo, W.; Kleitz, F.; Ryoo, R. *Chem. Commun.* **2003**, 1340.
(41) Laha, S. C.; Ryoo, R. *Chem. Commun.* **2003**, 2138.
(42) Cho, J.; Kim, Y. W.; Kim, B.; Park, B. *Angew. Chem., Int. Ed.* **2003**, *42*, 1618.
(43) Lee, H.; Kim, M. G.; Cho, J. *Electrochem. Commun.* **2007**, *9*, 149.

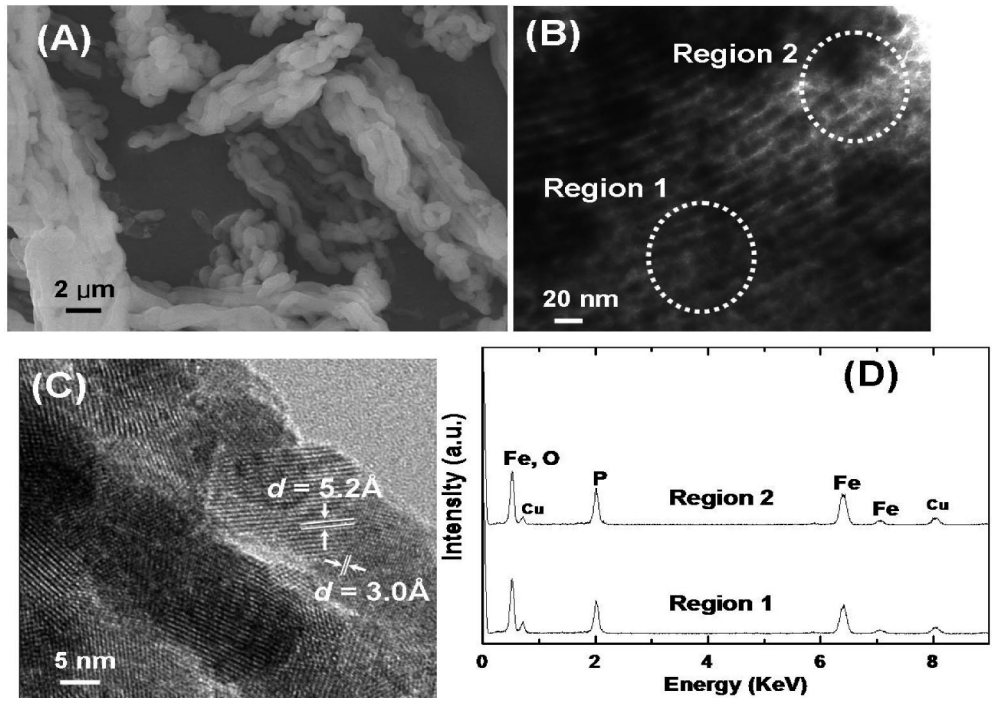

Figure 1. (A) TEM images of $LiFePO_4$ nanowires. (B) TEM image of (A). (C) is an expanded image of (B). (D) EDX spectra of regions 1 and 2 in (B).

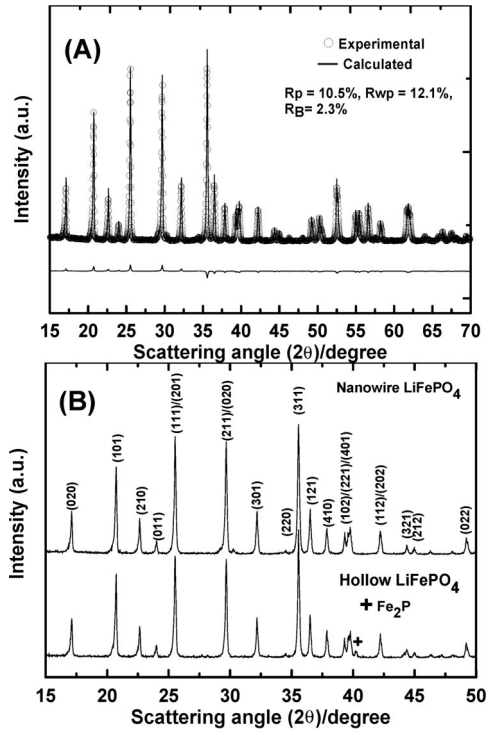

Figure 2. (A) Rietveld refinement of the nanowire $LiFePO_4$ powder and (B) XRD patterns of the nanowire and hollow $LiFePO_4$ prepared via a third impregnation and coating, respectively.

contents of the nanowire and hollow samples were estimated to 0.41 and 0.43 wt %, respectively.

To prepare the nanowire $LiFePO_4$, the same transparent $LiFePO_4$ precursor solution used for preparing the hollow sample was heated at 40 °C for 30 min until a viscous gel solution was formed. The gel solution was then mixed on the silica template, followed by drying, template removal, and firing. An XRD diffraction pattern of this sample confirms the formation of crystalline $LiFePO_4$, showing an orthorhombic olivine structure with a *Pnma* space group (a = 10.333(2), b = 6.005(3), and c = 4.701(4)) (Figure 2). The unit cell volumes of the synthesized hollow and nanowire samples were 291.82 and 291.69 $Å^3$, respectively, which are similar to the values reported in the literature.[19,21] Rietveld refinement results showed that the crystallite sizes of the nanowire and hollow samples were similar to each other, approximately 20 nm. Hence, Yamada's model,[44] dealing with relationship between the miscibility gap of the $LiFePO_4$ and its particle size, cannot be applied in our samples.

Figure 3A shows a typical SEM image of the hollow sample, and clusters of hollow $LiFePO_4$ particles with wall thicknesses of ~20 nm (Figures 3B and 3C) were obtained. Hollow metal or metal oxides were obtained from the hollow samples just after template removal at room temperature or <400 °C,[32–39] and therefore their original morphologies were sustained. However, $LiFePO_4$ is required to fire the samples after removal of the templates at 700 °C to enhance its crystallinity. Thus, its morphology was rather distorted and aggregated as shown in SEM image (A). Figure 3D shows energy-dispersive X-ray (EDX) spectra of regions 1 and 2 in the hollow sample after the first coating, followed by annealing at 300 °C, template etching, and annealing at 700 °C. It shows no trace of Si and Na, confirming that no reaction with the silica template occurred at 300 °C, but ICP-MS showed that residual Si and Na contents after firing were 15 and 23 ppm, respectively. Figures 3E and 3F show electron diffraction patterns of the wall region of (B) along the [101] direction along with a high-resolution image of

(44) Yamada, A.; Koizumi, H.; Nishimura, S.-I.; Sonoyama, N.; Kanno, R.; Yonemura, M.; Nakamura, T.; Kobayashi, Y. *Nat. Mater.* **2006**, *5*, 357.

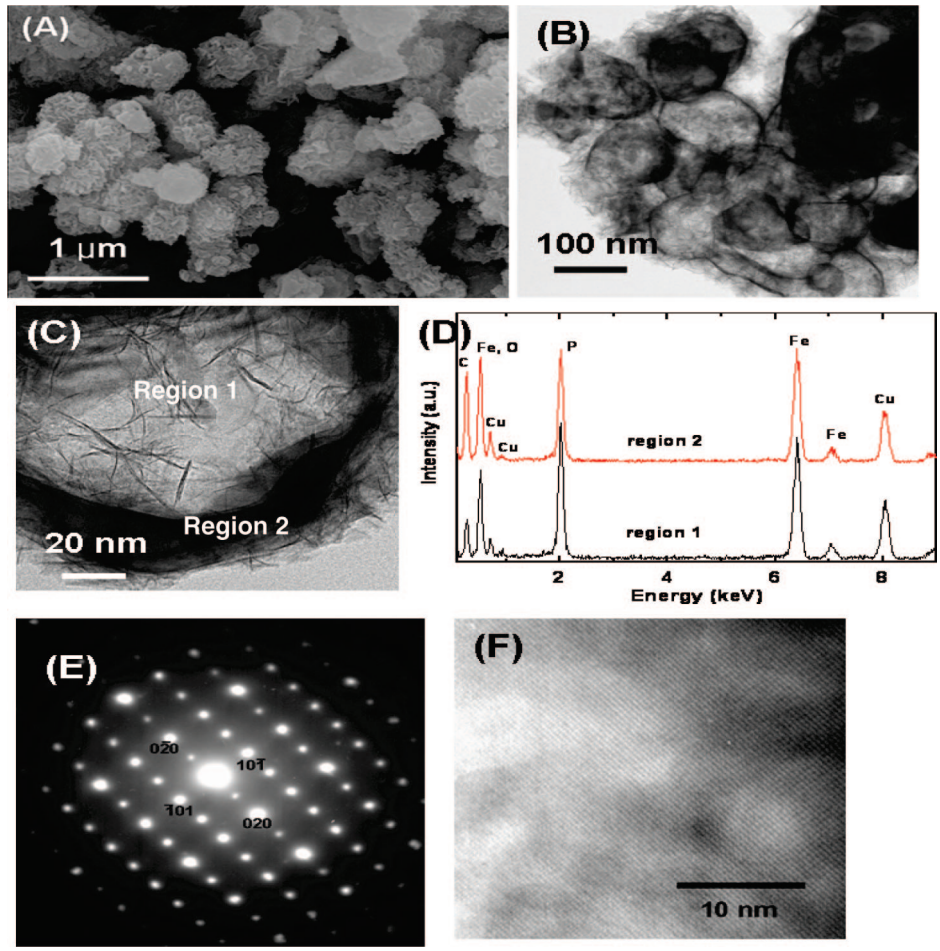

Figure 3. (A and B) SEM and TEM images of hollow $LiFePO_4$, respectively. (C) Magnified TEM image of (B). (D) EDX spectra of regions 1 and 2 in (C). (E) Electron diffraction pattern of (E) along the [101] zone axis. (F) High-resolution TEM image of (E) along the [110] zone axis.

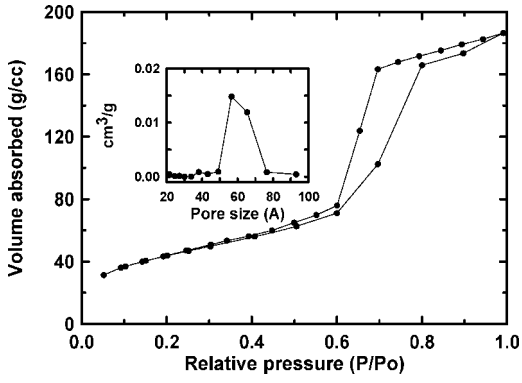

Figure 4. Nitrogen adsorption−desorption isotherms at 77 K of hollow $LiFePO_4$. The inset is the pore size distribution of hollow $LiFePO_4$.

(E) along the [110] direction, which confirm the formation of single-crystalline hollow $LiFePO_4$ particles.

Figure 4 exhibits N_2 adsorption and desorption isotherms of the hollow sample, which have a well-defined step for the relative pressure P/P_o ranging from 0.6 to 0.8, which is characteristic of mesoporous material. Barrett−Joyner−Halenda (BJH) analysis (inset) confirms well-ordered mesoporous tin phosphate with a pore size of 5.6 nm. Its BET specific surface area is 103 m^2/g, and it is higher than other mesoporous lithium metal oxides, such as $LiCoO_2$[13] and $LiMn_2O_4$.[45] These results indicate that a large surface area facilitates larger contacts areas for the electrolyte contacts with mesoporous hollow shell frameworks, resulting in fast Li ion mobility and lower charge-transfer resistance, in turn, reducing the local current density for a given total operating current. On the other hand, the Brunauer−Emmett−Teller (BET) surface area of the nanowire sample was 45 m^2/g.

Charge and discharge profiles obtained from coin-type cells containing nanowire and hollow $LeFePO_4$ cathodes with increasing C rates from 0.2C (=32 mA/g) to 15C between 2 and 4.2 V are presented in Figures 5A and 5B (identical charge and discharge rates were used). The Coulombic efficiency of the first cycle in the nanowire sample is 94%, and the first discharge capacity is 157 mA·h/g at a 0.2C rate. Furthermore, the discharge capacity at a rate of 15C shows 137 mA·h/g, corresponding to a capacity retention of 89%, compared with the capacity at a rate of 0.2C. Even after repetitive cycles at a 15C rate, negligible capacity fade is observed; full recovery of the capacity was observed when the C rate was decreased to 0.2C (Figure 6A). The rate capability of the electrode materials significantly depends on the loading level of the active materials; in this case a relatively high loading level of 30 mg/cm^2 (only active material) and electrode thickness of 30 μm were used to investigate the rate capability at higher C rates. When the loading level was decreased to 15 mg/cm^2, the capacity at

(45) Luo, J.-Y.; Wang, Y.-G.; Xiong, H.-M.; Xia, Y. *Chem. Mater.* **2007**, *19*, 4791.

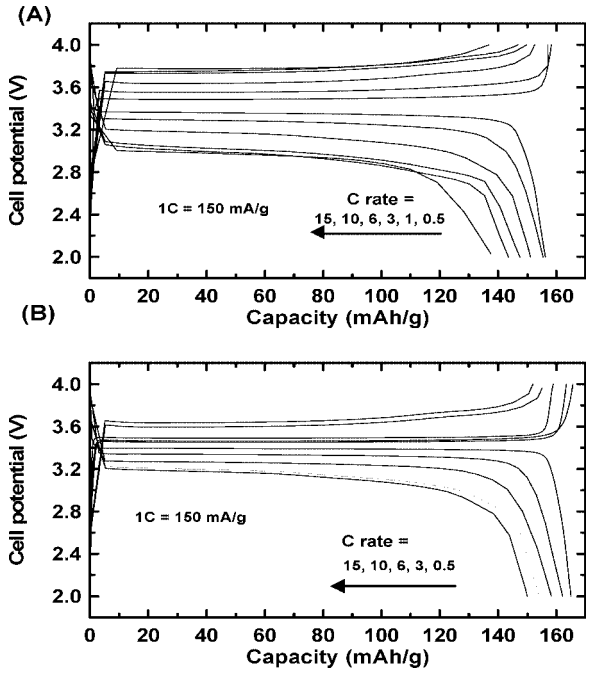

Figure 5. Voltage curves of (A) nanowire and (B) hollow $LiFePO_4$ at different C rates from 0.2 (=32 mA/g) to 15C (=2400 mA/g) between 4 and 2.0 V in coin-type half-cells (identical charge and discharge rates were used).

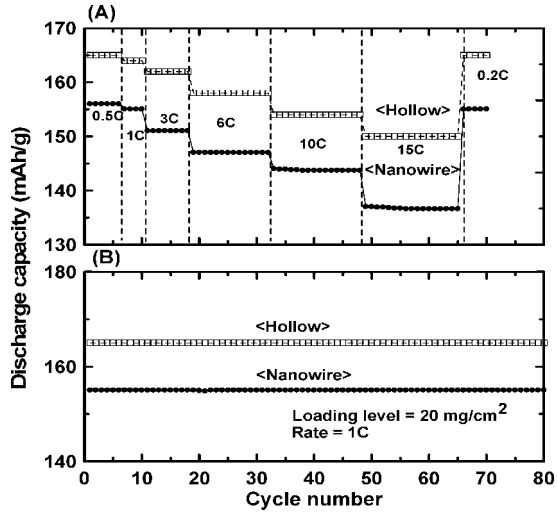

Figure 6. (A) Plot of the discharge capacities vs the cycle number at different C rates in hollow and nanowire $LiFePO_4$. (B) Plot of the discharge capacities vs the cycle number at a 1C rate in hollow and nanowire $LiFePO_4$, respectively.

the 15C rate was 147 mA·h/g, showing 96% capacity retention compared with the capacity at a 0.2C rate. Figure 6B depicts the discharge capacity of the nanowire at a loading level of 20 m^2/g as a function of cycle number up to 80 cycles; it shows no capacity fade. Furthermore, there is no capacity fading after 80 cycles at a 1C rate.

In contrast, due to the enhanced electrolyte contact area of the hollow $LiFePO_4$cathode with the electrolytes, the hollow sample shows its first discharge capacity of 165 mA·h/g (Figure 5B), which is higher than that of the nanowires. Additionally, the rate capability of the hollow sample exhibits a greatly improved value, showing 153 mA·h/g at 15C, which corresponds to a 95% capacity retention, compared to that at 0.2C (Figure 6A). The capacity retention at 15C was improved by 6%, compared to that of the nanowires. However, similar to the nanowires, full capacity recovery to 165 mA·h/g is observed at 0.2C rate cycling even after continuous 15 C rate cycles. Similar to the nanowire, there is no capacity fading after 80 cycles at a 1C rate (Figure 6B). The presence of conductive carbon and/or Fe_2P phases in the two types of $LiFePO_4$ samples may contribute to the observed high-rate capabilities. The higher surface area of the hollow sample, which decreases the effective current density during discharge compared to that of the nanowires, further enhances its high power performance.

4. Conclusions

Our results demonstrated that manipulation of the nanostructures provides versatile strategies toward improving the electrochemical properties at higher C rate. It was demonstrated that highly crystalline nanowires and hollow lithium-containing nanostructures could be prepared using the SBA-15 and KIT-6 templates method, which consists of forming a $SiO_2/LiFePO_4$ composite at 300 °C and removing the template, followed by further annealing at 700 °C. Electrochemical cycling data of both the nanowire and hollow $LiFePO_4$ at high C rates showed excellent capacity retention even at 15C rate cycles, with over 89% capacity retention. The volumetric energy density of the mesoporous and nanowire $LiFePO_4$ is expected to be decreased, compared to its solid counterpart. However, our results clearly demonstrated higher power density at higher current rates than those of previously reported solid counterparts.

Acknowledgment. This work was supported by the IT R&D program of MKE/IITA (Core Lithium Secondary Battery Anode Materials for Next Generation Mobile Power Module, 2008-F-019-01).

CM8006364